Clinical and Experimental HYPERTENSION

http://informahealthcare.com/ceh
ISSN: 1064-1963 (print), 1525-6006 (electronic)

Clin Exp Hypertens, Early Online: 1–8
© 2013 Informa Healthcare USA, Inc. DOI: 10.3109/10641963.2013.789047

informa healthcare

Tempol blunts afferent arteriolar remodeling in chronic nitric oxide-deficient hypertension without normalizing blood pressure

Rodrigo O. Marañon[1,2,3], Luis A. Juncos[1,3], Claudio Joo Turoni[2], Sofia Karbiner[2], Damian Romero[4], and María Peral de Bruno[2]

[1]*Department of Physiology and Biophysics, University of Mississippi Medical Center, Jackson, MS, USA,* [2]*Department of Physiology and Bioengineering, INSIBIO, Universidad Nacional de Tucumán, Tucumán, Argentina,* [3]*Department of Medicine/Nephrology, and* [4]*Department of Biochemistry, University of Mississippi Medical Center, Jackson, MS, USA*

Abstract

Background/Aim: Renal preglomerular vessels play a central role in modulating renal function and injury, especially during conditions of renal hemodynamic stress such as hypertension. We evaluated whether improving the balance between nitric oxide (NO) and oxidative stress improves the morphological alterations of renal afferent arterioles that occur in NO deficiency-induced hypertension.
Methods: We measured indices of NO and oxidative stress and evaluated renal morphology and afferent arteriolar remodeling in rats treated with vehicle, L-NAME or L-NAME plus tempol (a superoxide dismutase mimetic) for 6 weeks.
Results: L-NAME-treated rats had hypertension, lower urinary and renal NO indices, higher renal cortical levels of TBARS, GSSG and GSSG/GSH. This was associated with significant eutrophic inward remodeling of the afferent arterioles; they had a marked decrease in arteriolar lumen area and a striking increase in arteriolar wall thickness and media to lumen ratio. Tempol did not significantly reduce blood pressure, but increased NO levels, decreased oxidative stress and partially blunted L-NAME-induced remodeling of afferent arterioles.
Conclusion: L-NAME-induced remodeling of afferent arterioles is blunted by tempol. This beneficial effect on remodeling is associated with increases in NO indices, decreases in oxidative stress, without significant decreases in blood pressure. Thus, the balance between these components may contribute to the altered renal hemodynamics and function in this model.

Keywords

Afferent arteriole, hypertension, nitric oxide, oxidative stress, remodeling

History

Received 27 December 2012
Revised 12 February 2013
Accepted 19 February 2013
Published online 20 June 2013

Introduction

The kidney plays a central role in the pathogenesis of human and experimental hypertension (1–3) and does so by various means including tubular and vascular mechanisms. Among the vascular mechanism, increased renal vascular resistance (particularly of the preglomerular arterioles) has been reported in various experimental and human models (4–7), even in the prehypertensive state. While the increased vascular resistance may be due to enhanced vascular reactivity (8), there is growing evidence that the hemodynamic changes associated with hypertension are associated with alterations in the structure of the renal resistance vessels (9). For instance, renal afferent arterioles of spontaneously hypertensive rats (SHR) have hypertrophy, a decrease in luminal diameters and in the cross-sectional area of the media (10–12). Such vascular remodeling has also been found in angiotensin II-dependent hypertensive models (13). This thickening of the wall vessel is thought to constitute a compensatory mechanism to normalize the wall tension; thus, wall tension would be the primary biological signal driving the vascular remodeling (14,15). Indeed, various studies including our own have found that decreasing blood pressure blunts vascular remodeling in hypertensive rats (16). However, vascular remodeling of the preglomerular arterioles can also be found in the absence of hypertension. For instance, there is marked preglomerular vascular remodeling in streptozotocin-induced diabetic rats (17) and in an experimental model of metabolic syndrome (18), despite the absence of hypertension. Consequently, these studies suggest that other factors, such as hormonal and/or metabolic factors, may also contribute to remodeling of the renal microvasculature. In this respect, much attention has been focused on the renin-angiotensin system. However, alterations in the NO bioavailability are also an important determinant in cardiovascular remodeling.

Endogenous NO is a key factor in regulating blood pressure and cardiovascular remodeling in experimental hypertension models and humans (19,20). It blunts the

Correspondence: María Peral de Bruno, PhD, Department of Physiology and Bioengineering, INSIBIO, Universidad Nacional de Tucumán, Tucumán. Balcarce 32 S. M. de Tucuman, Tucuman, (4000) Argentina. Tel: 54-381-4307331. E-mail: mperal@ct.unt.edu.ar

proliferative response of vascular smooth muscle cells (VSMCs) during remodeling stimuli. Thus, decreases in the NO bioavailability (via either decreased production or increased destruction) not only causes endothelial dysfunction and hypertension, but may also promote abnormal remodeling or enhance hypertension-induced remodeling (21). Indeed, treating rats with the NO synthase inhibitor, N^{ω}-nitro-L-arginine methyl ester (L-NAME), causes endothelial dysfunction, renal vasoconstriction and hypertension (22), as well as marked renal vascular injury and remodeling consisting of increased cell proliferation, macrophage infiltration and accumulation of lipid/low-density lipoproteins in the preglomerular arterioles (23), and thickening of the wall of the intrarenal resistance vessels (24).

It is important to note that inhibiting NO production also results in enhanced generation of superoxide anion (25), which in turn may further decrease NO and produce a detrimental feedback loop that results in an augmentation of hypertension, as well as worse renal vascular remodeling and injury. However, the impact of this interaction between NO, oxidative stress and blood pressure in determining L-NAME-induced preglomerular vascular remodeling are not yet clear. Therefore, the objective of this study was to examine the role of oxidative stress in determining renal cortical NO levels, afferents arteriolar remodeling and blood pressure in L-NAME-induced hypertension.

Material and methods

Experimental animals

All animal procedures were performed in accordance with Argentine law and performed in accordance with the Guide for the Care and Use of Laboratory Animals (NIH publication 92–93) and the Guidelines of the Animal Welfare Act. Male Sprague Dawley rats weighing 274.7 ± 20.3 g were randomized into three groups all containing 10 rats. Group 1 (control rats) was maintained on standard rat chow and water, group 2 (L-NAME rats) received L-NAME (50 mg/kg/day for 6 weeks) in their drinking water and group 3 (L-NAME + tempol) received L-NAME and tempol (1 mMol for 6 weeks) in the same manner. Body weight, drinking water and food intake were measured daily. Twenty-four-hour creatinine clearances were obtained at the beginning of the protocol and after 6 weeks. The final 24-h urine collection was also used to measure urinary nitrites. Following the 6-week period, the rats were anesthetized with sodium pentobarbital (45 mg/kg intraperitoneally) and the right carotid artery cannulated for determination of the mean arterial pressure (MAP) and heart rate (HR). After determination of MAP and HR, the kidneys were perfused clear of blood with PBS, removed and weighed. Left kidneys were used for histological/morphological analysis and immunohistochemistry according to the technique described in previous studies from our laboratory (17,26), and right kidneys were used for measurement of NO, nitrites, lipid peroxidation and glutathione.

Renal histological analysis

To obtain a maximum dilation of the afferent arterioles, the vessels were perfused with PBS continuously for 10 min at 100 mmHg. The PBS-perfused kidneys were placed into 5–20 time volume of 10% buffered formalin, after which they were embedded in paraffin, sliced into 3-μm sections (Sagittal sections through the widest diameter) and subjected to hematoxylin-eosin (H&E) or periodic acid Schiff (PAS) staining. Analysis with light microscopy at 400 x (Olympus CH30) was performed to assess pathological changes.

Morphological analysis

First, the glomerular number and density (ratio of kidney area/number of glomeruli) was determined by counting the number of glomeruli in a whole-kidney section. This procedure was repeated three times per kidney in order to measure the glomerular area, Bowman's space and surface area of preglomerular vessels by a stereological method and the average was recorded. Then, the remodeling of afferent arterioles was evaluated. For this, lumen area, media thickness, media/lumen ratio and cross-sectional area of afferent arterioles were quantified using a stereological method (26). Afferent arterioles were identified by their location adjacent to the vascular pole of the glomerular tuft, by the presence of an internal elastic lamina and by having fewer thin flattened endothelial cells than the efferent arteriole. All afferent arterioles of a whole-kidney section were counted and the procedure was repeated three times per kidney and the average was recorded. Images of the sections were captured using a video camera (SONY DXC-390P Camera, Sony Corporation, Tokyo, Japan) connected to the light microscope which was connected to an informatics system. The images were studied off line with the program Image J 1.43 μ. For this purpose, images were converted to RGB files in order to evaluate separately the signals of three colors (red, green and blue). Previously, each pixel was calibrated to correspond to an equivalent μm^2 value. Histogram was performed to study area and the area was measured with the freehand selection tool, keeping only the pixels that coincided with the histogram. Each vessel was measured three times and the average was recorded.

Immunohistochemistry

We evaluated vascular smooth muscle cell (VSMC) density and the presence of the endothelial layer in the afferent arterioles using anti-α actin-specific antibody (Dako North America, Carpinteria, CA) and anti-CD31-specific antibodies (Sigma-Aldrich Corporation, St. Louis, MO). Kidney paraffin sections (3 μm) were deparaffinized in xylol and rehydrated in a graded alcohol series. Endogenous peroxidase was inhibited with H_2O_2 (3% in methanol). Sections were then washed in distilled water and heated in citrate buffer 10 mM (pH 7.0) for 15 min. Slides were incubated first with normal goat serum for 5 min and then with antibodies (dilution: 1/160) for 30 min at 20 °C. Next, slides were incubated in a Link L Label IHC detection system (BioGenex, Fremont, CA). Antibody binding was revealed using JHC expressing H_2O_2 as a substrate and diaminobenzidine (DAB) as the chromogen (Liquid DaB; BioGenex, Fremont, CA). Counterstaining was performed with

hematoxylin. Positive controls consisted of immunohistochemistry visualization of antibodies anti-α actin-specific antibody stained VSMCs (27) and anti-CD31 stained endothelial layer. Afferent arterioles were identified by their histological features. Lastly, we determined the type of remodeling (hypertrophy or hyperplasia) of the smooth muscle cell layer of afferent arterioles. For this, the ratio between density of anti-α actin-stained area and number of H&E-stained VSMCs nuclei was calculated in serial sections (28). Histological findings, immunohistochemistry staining and the density of anti-α actin staining area were measured using image analyzer software (ImageJ 1.43u, National Institutes of Health, Bethesda, MD).

Assessment of nitric oxide

Urinary nitrites

Twenty-four hour urinary nitrite excretion was measured as an indirect index of *in vivo* NO production using the Griess reaction. Briefly, NO metabolites were transformed into diazoic-colored compounds by adding N-(l-naphthyl) ethylenediamine (50 µl, 0.2%) and sulfanilamide (450 µl, 0.1%) to each tube containing standard or experimental samples. Absorbance was measured at 540 nm with a spectrophotometer (SPECTRUM, SP-1103 Spectrophotometer, China). Nitrite absorbance was calculated with linear regression analysis. Regressions with a correlation coefficient >0.95 were used.

Renal tissue nitrites

For calculation of nitrites in renal tissue, cortex samples (60 ± 6 mg) were placed in Eppendorf tubes with 0.5 ml of Krebs solution bubbled with 95% O_2 and 5% CO_2 at a pH of 7.4 at 37 °C. The samples were allowed to equilibrate for 30 min after which nitrites were measured using the Griess reaction as described above. To test whether reactive oxygen species were altering nitrite contents in the tissue samples, separate experiments in which the tissue samples were treated with a SOD mimetic (tempol; 10^{-5} M for 30 min) were performed. After which the nitrite content was determined by the Griess reaction. Non-NOS NO production was determined by measuring nitrites in tissues samples that had been incubated for 30 min with 10^{-4} M L-NAME.

Direct measurement of NO

NO release directly measured from the harvested renal tissue samples was also performed using an NO-sensitive electrode (ISO-NOP Sensor, World Precision Instruments, Inc, Sarasota, FL). This membrane-type NO-sensitive electrode consists of a working electrode covered by a gas-permeable polymeric membrane. NO diffuses through the selective membrane or coatings and is oxidized on the surface of the pre-polarized electrode, resulting in an electrical current. The magnitude of the redox current is in direct proportion to the concentration of NO in the sample and is amplified by the NO meter and registered by a computer (Apollo 4000 recording system; World Precision Instruments, Inc, Sarasota, FL). The selectivity of the NO-sensitive electrode was tested in connection with calibration, where a lack of response to strong saline solution (3 mol/L) or sodium nitrite ($NaNO_2$) up to 100 µmol/L was taken as an evidence for an intact coating of the electrode. The electrode was calibrated by chemical titration based on the following equation: $2KNO_2 + 2KI + 2H_2SO_4 \rightarrow 2NO + I_2 + 2H_2O + 2K_2SO_4$, where a known amount of KNO_2 is added to produce a known amount of NO. The NO electrode was connected to the amplifier, and the signals were recorded and the calibration curve was performed. After the calibration procedures, NO was measured in the renal cortical tissue (63 ± 5 mg) by inserting the electrodes into tissue samples that were placed in acrylic chambers. After 60 to 120 min of equilibration in the organ chamber, the electrode was stabilized and the baseline of the current became stable. NO was determined continuously throughout the experiment. The impact of oxidative stress and NOS on NO levels was determined by performing separate studies, in which NO production was measured in tissue samples from each group treated with either tempol or L-NAME as described above.

Assessment of oxidative stress

Oxidative stress equilibrium was calculated by measuring lipid peroxidation and glutathione. Lipid peroxidation was evaluated using the thiobarbituric acid method (29). Briefly, cortex fractions were homogenized in detergent-free buffer. Next, EDTA 1 mM (Sigma, St. Louis, MO) was added to 0.1 ml homogenates and 20% trichloroacetic acid (1 ml) was added to precipitate proteins. The homogenates were centrifuged at 15 000 rpm for 15 min at 4 °C to separate the membranes (pellet) and cytosolic fractions (supernatant). The supernatant was then treated with 0.5% thiobarbituric acid (1 ml) in a boiling water bath for 60 min. After cooling, the absorbance was read at 535 nm in a spectrophotometer (Beckman DU 7500 Spectrophotometer, Beckman Instruments, Inc., Fullerton, CA). The concentration of thiobarbituric reactive substances (TBARS) was calculated using malondialdehyde (MDA) as a standard. Results were expressed as µmol TBARS/mg of protein. The homogenate protein content was determined by the Lowry method (30).

Total free glutathione and reduced glutathione (GSH) were determined by modifying a spectrophotometric procedure (31). To determine total glutathione content, cortex fractions were homogenized in phosphate buffer plus EDTA 6.3 mM (Sigma, St. Louis, MO) (pH 7.4). Then, 0.2 ml of each homogenate was mixed with 10% trichloroacetic acid (0.2 ml) to precipitate proteins. The homogenates were centrifuged at 12 000 rpm for 15 min at 4 °C. Next, 20 µl of the supernatant was incubated with NADPH 0.3 mM (0.7 ml) and DTNB 6 mM (0.1 ml) in a water bath for 2 min (30 °C). Finally, glutathione reductase 0.077 U (10 µl) was added. The absorbance was read at 412 nm in a spectrophotometer (Beckman DU 7500 Spectrophotometer, Beckman Instruments, Inc., Fullerton, CA) after 35 min. To determine GSH, 20 µl of the supernatant was incubated with DTNB 6 mM (0.1 ml), and the absorbance was read at 412 nm at 15 min. The oxidized glutathione (GSSG) was calculated by subtracting the amount of GSH from the total amount of glutathione. Results were correlated with protein content determined by the Lowry method, and GSSG/GSH ratios were calculated.

Statistical analysis

Results were expressed as mean ± standard error. Statistical analyses were performed with STATISTICA 5.0 software (StatSoft, Tulsa, OK). For statistical comparison, ANOVA was used with Newman–Keuls test when appropriate. Results were considered significant when $p < 0.05$.

Results

General and morphological characteristics

The general characteristics of control, L-NAME and L-NAME plus tempol rats are shown in Table 1. L-NAME rats had a markedly elevated MAP. Although tempol showed a tendency to decrease the blood pressure, the values were not significantly different than the L-NAME group. Neither L-NAME nor L-NAME plus tempol altered the rat's body weight, food intake, heart rate, creatinine clearance or kidney weight.

Although there were no differences in the kidney weight, the morphological findings in the kidney were significantly altered by the treatments. Glomerular number, density, size and the number of nuclei per glomerulus were all decreased by L-NAME (Table 2); tempol did not prevent any of these L-NAME-induced changes (Table 2). L-NAME also caused glomerular congestion, retraction of the glomerular tuft, hyaline deposits, occasional fibrinoid necrosis and reduction of Bowman's space (Control rats: 102.5 ± 5.6, $n = 8$ versus L-NAME rats: $19.27 \pm 2.2\,\mu m^2$, $n = 6$; $p < 0.001$). Tempol treatment blunted L-NAME-induced reduction in Bowman's space so that the values approached that of controls ($89 \pm 9.3\,\mu m^2$, $n = 6$; p: NS).

Figure 1 shows microphotographs that portray vascular remodeling of afferent arterioles control, L-NAME and L-NAME plus tempol, whereas Figure 2 shows the summarized data of (A) media thickness, (B) lumen area, (C) media/lumen ratio and (D) Cross-sectional area of afferent arterioles. Afferent arterioles of L-NAME showed media thickening, decreased lumen area and alteration of the media/lumen ratio compared to controls. Tempol was able to blunt L-NAME-induced vascular remodeling in afferent arterioles, but not normalize it. No significant difference was found in the cross-sectional area in afferent arterioles of control, L-NAME and L-NAME plus tempol ($43.1 \pm 7.8\,\mu m^2$, $n = 8$; $57.4 \pm 4.4\,\mu m^2$, $n = 6$ and $50.4 \pm 3.5\,\mu m^2$, $n = 6$, respectively; p: NS). To assess whether the remodeling was due to hypertrophy and/or hyperplasia of the VSMC, we determined the intensity of actin staining in the media of afferent arterioles and counted the number of H&E-stained VSMC nuclei (to calculate the actin-stained area/number of nuclei ratio). L-NAME increased the intensity of actin staining and the ratio of actin-stained area/number of nuclei (control: 0.71 ± 0.2, $n = 6$ versus L-NAME 12.86 ± 5.1, $n = 6$;

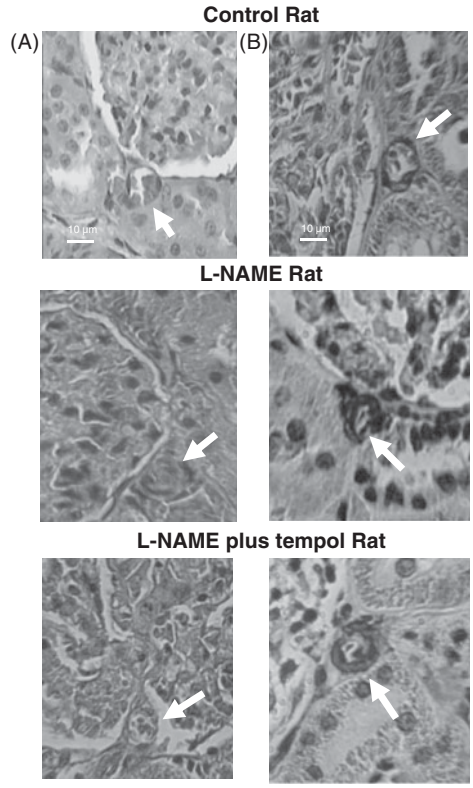

Figure 1. Effect of tempol on L-NAME-induced vascular remodeling of renal afferent arterioles. Left Panel (A): Microphotograph (600X) of the H&E-stained renal cortex of Control, L-NAME and L-NAME plus tempol-treated rats. Right Panel (B): Microphotograph (600X) of the afferent arteriole (arrows) stained with anti-α actin antibody. Afferent arterioles are indicated by arrows. Note the presence of inward eutrophic remodeling that is present in the afferent arterioles of the L-NAME-treated rats. Tempol blunted L-NAME-induced remodeling of the afferent arterioles; it decreased thickening of the vascular wall and improved the wall-to-lumen ratio.

Table 1. Characteristics of control, L-NAME and L-NAME plus Tempol.

Rat	Body weight (g)	Food intake (g/24 h)	MAP (mmHg)	Heart rate (bmp)	Kidney weight (g)	Creatinine clearance (ml/min)
Controls	282 ± 9 ($n = 10$)	27.0 ± 7.8 ($n = 10$)	108 ± 2 ($n = 10$)	367 ± 3 ($n = 8$)	1.1 ± 0.1 ($n = 10$)	0.5 ± 0.1 ($n = 9$)
L-NAME	280 ± 6 ($n = 10$)	24.6 ± 3.8 ($n = 10$)	177 ± 9* ($n = 10$)	365 ± 3 ($n = 9$)	1.1 ± 0.2 ($n = 10$)	0.6 ± 0.2 ($n = 7$)
L-NAME + Tempol	276 ± 6 ($n = 10$)	25.3 ± 7.1 ($n = 10$)	165 ± 7* ($n = 8$)	367 ± 2 ($n = 8$)	1.0 ± 0.2 ($n = 7$)	0.7 ± 0.2 ($n = 6$)

MAP: Mean arterial pressure. Values represent means ± standard error. *$p < 0.001$ versus Control

Table 2. Glomerular characteristics of control rats, L-NAME rats and L-NAME plus Tempol.

Rat	Glomerular number	Glomerular density	Glomerular size	Number of nuclei per glomerulus
Control	256 ± 10 ($n = 10$)	5.9 ± 0.2 ($n = 10$)	295 ± 6 ($n = 10$)	66.0 ± 5.1 ($n = 10$)
L-NAME	180.4 ± 12** ($n = 10$)	4.2 ± 0.3** ($n = 9$)	179 ± 18* ($n = 9$)	41.3 ± 3.1** ($n = 9$)
L-NAME + Tempol	167 ± 3** ($n = 7$)	4.8 ± 1.1** ($n = 7$)	209 ± 13* ($n = 7$)	49.6 ± 5.3** ($n = 7$)

Values represent means ± standard error. n: number of animals within brackets. **$p < 0.01$ versus Control; *$p < 0.05$ versus Control.

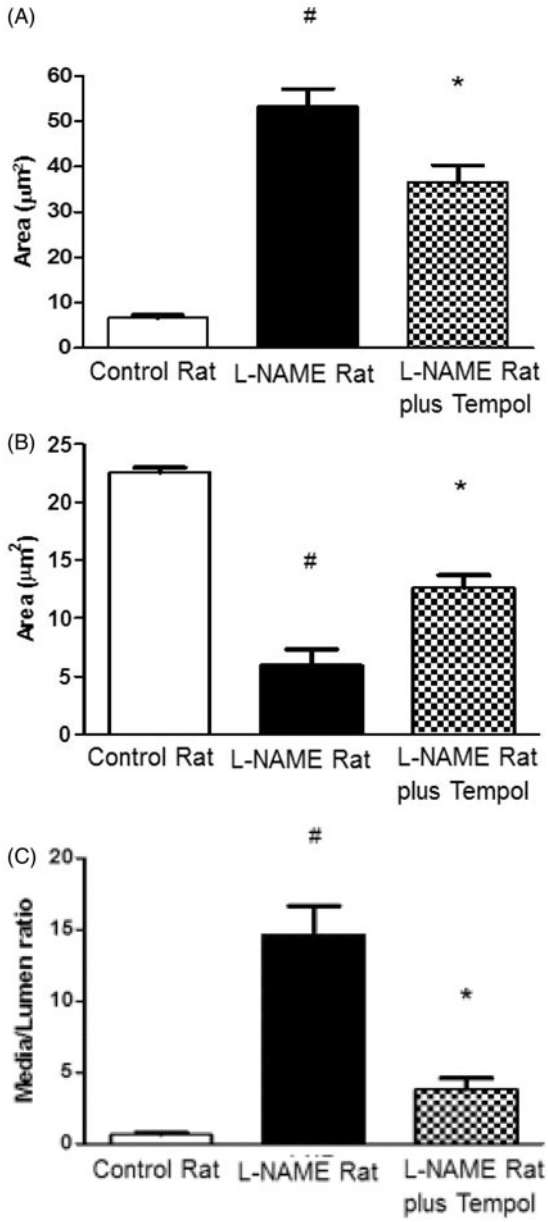

Figure 2. Stereological comparison of afferent arteriolar media thickness (A), lumen area (B) and media/lumen ratio (C) in control, L-NAME and L-NAME plus tempol-treated rats. L-NAME increased the thickness of the vascular media and decreased the luminal area, resulting in an increased media/lumen ratio. Tempol blunted all of these L-NAME-induced vascular changes. #$p<0.001$ L-NAME versus Control and *$p<0.01$ L-NAME plus tempol versus Control.

$p<0.001$). Tempol did not alter L-NAME-induced actin staining nor the ratio of actin-stained area/number of nuclei (11.38 ± 6.1, $n=6$), suggesting that tempol did not alter L-NAME-induced hyperplasia.

Nitric oxide indices

Urinary nitrite excretion was measured as an indirect measures of *in vivo* NO status (Figure 3). Urinary nitrite levels were higher in control than L-NAME rats (5.6 ± 2.2 versus 0.2 ± 0.08 nmol/L, respectively). Tempol blunt decreased urinary nitrites in L-NAME-induced rats, but they remained significantly lower than the control levels (1.3 ± 0.4 nmol/L, Figure 3).

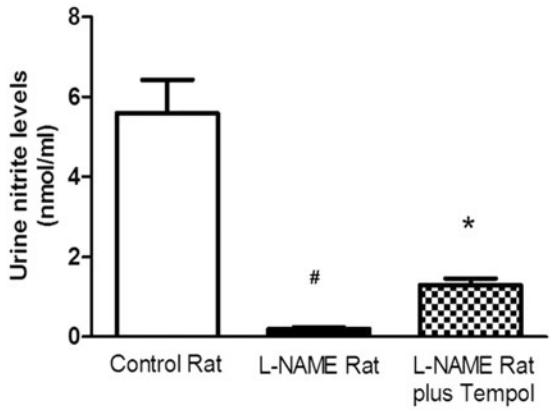

Figure 3. Urinary nitrite levels in control, L-NAME and L-NAME plus tempol-treated rats. Tempol blunted L-NAME-induced reductions in urinary nitrite excretion. *$p<0.01$ versus Control and #$p<0.001$ versus Control.

Because urinary nitrite levels may not be representative of renal NO levels, we also measured NO indices in renal tissue. Figure 4(A) depicts renal cortical nitrite levels. As with urinary nitrites, L-NAME caused a profound decrease in renal nitrites (Control rats: 2.7 ± 0.4, $n=8$ versus L-NAME rats: 0.6 ± 0.1 pmol/mg tissue, $n=6$); this decrease in nitrites was significantly less when tempol was added to the incubation bath, suggesting that oxidative stress was quenching NO in the L-NAME but not control rats (Control rats: 2.6 ± 0.4, $n=8$ versus L-NAME rats: 1.9 ± 0.4 pmol/mg tissue, $n=6$). *In vivo* administration of tempol (L-NAME plus tempol rats) significantly blunted L-NAME-induced reductions in renal cortical nitrite levels, and addition of tempol to the incubation solution further blunted this so that the renal cortical nitrite levels now approached those of control rats; renal nitrite levels in the L-NAME plus tempol rats were 1.5 ± 0.3 and 2.5 ± 0.4 pmol/mg tissue ($n=6$) in the absence and presence of tempol in the incubation solution. Note that addition of L-NAME to the incubation solution nearly completely inhibited the release of nitrites from the renal tissue in the control and L-NAME plus tempol rats (data not shown), showing the measured nitrites were due to NO.

Because measuring NO indices such as nitrites have shortcomings, we further substantiated these results by directly measuring renal tissue NO levels using an NO-sensitive electrode. As shown in Figure 4(B), the changes in NO levels observed in response to L-NAME and L-NAME plus tempol (as measured with the NO-sensitive electrode) were essentially the same as those observed using the nitrites assays.

Oxidative stress

To examine the role of oxidative stress in this model, TBARS levels, total free glutathione and reduced glutathione in renal cortex of control rats, L-NAME rats and L-NAME plus tempol rats were measured. TBARS levels were significantly higher in L-NAME rats than control rats. Tempol blunted L-NAME-induced lipid peroxidation so that the levels approached that of control rats (Control rats: 0.58 ± 0.09 μmol/mg protein, $n=7$ versus L-NAME rats: 0.84 ± 0.06, $n=7$ and L-NAME plus tempol rats:

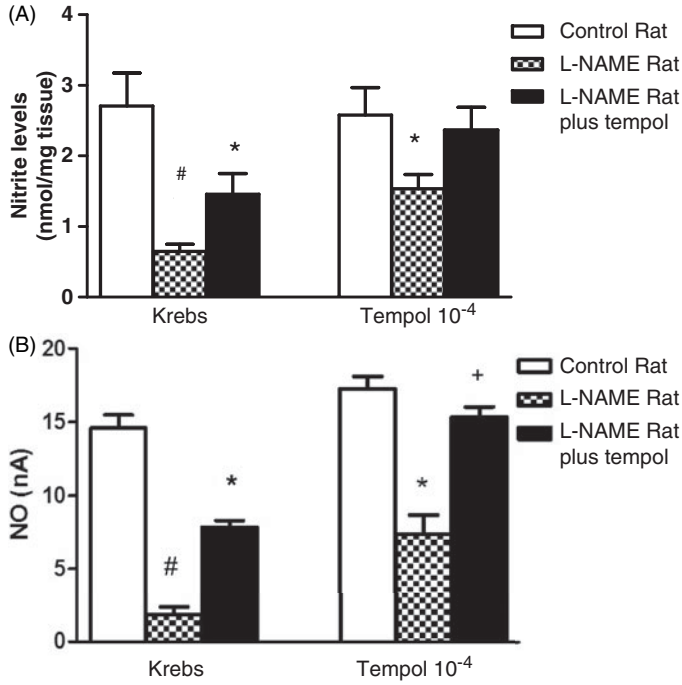

Figure 4. Nitrites (using a NO-sensitive electrode; Panel A) and direct NO measurements (Panel B) in the renal cortex of control, L-NAME and L-NAME plus Tempol-treated rats. Measurements were made in tissues bathed in Krebs solution or in Krebs solution containing tempol (10^{-5} M) to minimize post tissue collection (*in vitro*) increases in oxidative stress and its associated quenching of NO. #, $p<0.001$ versus Control; *, $p<0.01$ versus Control; and +, $p<0.05$ versus Control.

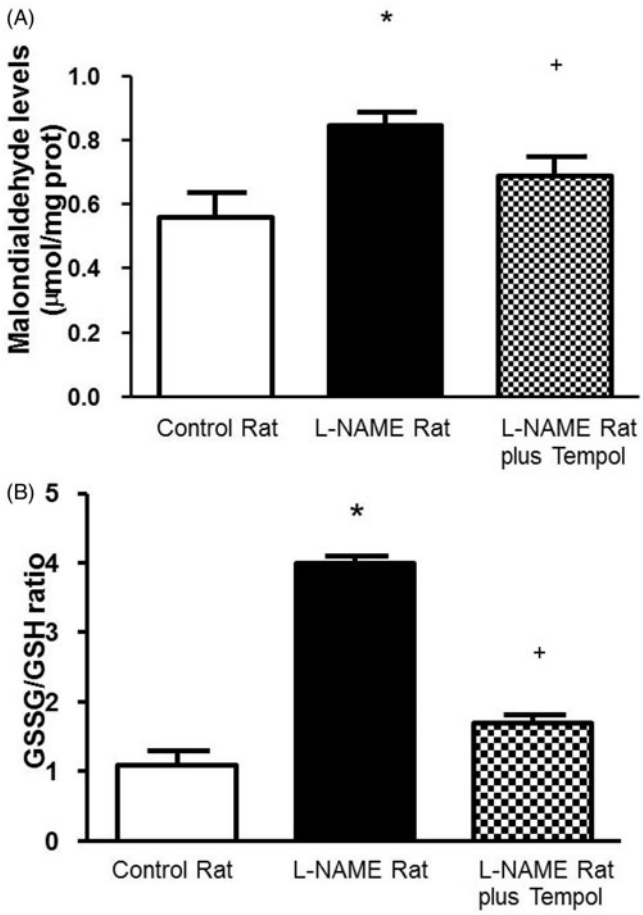

Figure 5. Quantification of oxidative stress in the renal cortical tissue homogenates of Control, L-NAME and L-NAME plus tempol-treated rats. Oxidative Stress was determined using two distinct measures: malondialdehyde levels (a measure of lipid peroxidation: Figure 5A) and the ratio of oxidized glutathione (GSSG)-to-reduced (GSH) (Figure 5B). Tempol attenuated L-NAME-induced increases in lipid peroxidation. *, $p<0.001$ L-NAME versus Control and +, $p<0.05$ L-NAME plus tempol versus Control.

0.67 ± 0.06, $n=6$; $p<0.01$; Figure 5A). Reduced glutathione (GSH) levels and GSSG/GSH ratio were lower in L-NAME rats than control rats and L-NAME plus tempol rats, and tempol blunts the effect of L-NAME treatment (GSH: Control rats: 11.5 ± 2.9 µmol/mg protein, $n=9$ versus L-NAME rats: 38.4 ± 8.1, $n=6$ and L-NAME plus tempol rats: 21.1 ± 4 µmol/mg protein, $n=6$; $p<0.01$; GSSG/GSH ratio: Control rats: 1.1 ± 0.6, $n=8$ versus L-NAME rats: 4.0 ± 0.1, $n=4$ and L-NAME plus tempol rats: 1.3 ± 0.3, $n=6$; $p<0.05$, respectively; Figure 5B).

Discussion

In general high blood pressure leads to vascular remodeling, a chronic adaptive process in which the wall of resistance vessels undergoes structural changes causing alterations in the thickness of the media and/or luminal area. While the mechanisms of these processes are not completely known, the available data indicate that it is not solely the result of elevated blood pressure; rather it is the result of the dynamic interaction between hemodynamic stimuli and biochemical/hormonal factors (32). For instance, angiotensin II, angiotensin 1–7, oxidative stress and NO all have important effects on vascular remodeling. NO is thought to attenuate the hypertension-induced vascular remodeling by decreasing blood pressure, modulating the effects of oxidative stress and inhibiting growth and proliferation of VSMCs. Blocking NO not only causes hypertension and prevents the anti-proliferative and anti-growth effects of NO on VSMCs, but also increases oxidative stress, which now exerts its vascular remodeling effects in an unopposed manner. We tested the role of oxidative stress in L-NAME-induced vascular remodeling. Our major findings are that tempol, an antioxidant agent, blunts L-NAME-induced remodeling, suggesting that oxidative stress plays a significant role in vascular remodeling in conditions of reduced NO. In addition, our results suggest that part of the effects of tempol may be independent of its blood pressure lowering effects.

Numerous studies have demonstrated the efficacy of chronic L-NAME administration in inducing hypertension and renal dysfunction (24,25). We found that 6 weeks of L-NAME in our rats caused marked reductions in urinary nitrite excretion and renal tissue NO, which were associated with a ~70 mmHg increase in blood pressure associated and significant alterations in renal morphology including marked vascular remodeling of the afferent arterioles. Remodeling can be hypertrophic (increase of cross-sectional area), eutrophic (no change in cross-sectional area) or hypotrophic (decrease of cross-sectional area) (33). The afferent arterioles in our L-NAME-treated rats exhibited increased media thickness with a decreased lumen area (thus resulting in a markedly increased media-to-lumen ratio) and no change in the cross-sectional areas of the arterioles. Moreover, the increased anti-α actin staining suggests an increase in VSMC mass. Taken together, these data suggest that the pattern of vascular remodeling of the afferent arteriole in the L-NAME-treated rats is most consistent with inward eutrophic remodeling (34). This pattern of vascular remodeling is similar to that reported in essential hypertension suggesting that it may simply be the result of increased blood pressure. However, other models of hypertension, such as the SHR, exhibit different modes of remodeling. Moreover, this remodeling could occur even in the absence of hypertension (e.g. diabetic rats), thus raising the possibility that other mechanisms may be implicated as well. In this respect, it is noteworthy that both essential hypertension and diabetes are associated with endothelial dysfunction and an increased oxidative stress. Thus it is tempting to speculate that the altered balance caused by decreased NO and increased oxidative stress may significantly contribute to the remodeling.

The role of oxidative stress on remodeling of the renal afferent arterioles during chronic NO inhibition has not previously been examined. In this study, we found that tempol, at a dose that reduces oxidative stress but does not significantly reduce blood pressure, blunted L-NAME-induced remodeling. These results suggest that oxidative stress plays an important role in L-NAME-induced vascular remodeling of renal afferent arteriole. Moreover, while we acknowledge that there may have been a small undetected difference in blood pressure contributing to these changes, it appears that the majority of the effect of tempol on vascular remodeling is largely independent of changes in blood pressure. Our results are consistent with those of Pires et al. (35), who showed that tempol prevents cerebral vessel remodeling in male SHR-SP model, independent of blood pressure changes. It is also interesting to note that tempol had a protective effect on renal vascular remodeling but not on the majority of the glomerular alterations. While the mechanisms for the differential effect of tempol on the renal microvasculature and glomeruli are unknown, it may be that a lower blood pressure may be required in order to afford glomerular protection. In addition, it is possible that the NO deficiency alters renal architecture by other pathways that are independent of oxidative stress. However, these possibilities require further studies.

The blood pressure-independent effects of tempol on vascular remodeling may have been due to withdrawal of the direct effects of oxidative stress on the vasculature. Indeed, we found that oxidative stress level to be markedly increased in the L-NAME-treated rats (as determined by TBARS and GSSG/GSH ratio) as has been reported previously. This increase in oxidative stress is associated with increased glomerular vascular resistance and remodeling (36). Thus, tempol-induced decreases in oxidative stress may directly impact this mechanism. However, an alternative explanation may be that tempol indirectly increases NO bioactivity (via the decrease in oxidative stress), which in turn exerts an anti-proliferative effect and consequently prevents vascular remodeling. While the remodeling of the afferent arterioles in this study was not associated with significant hyperplasia, tempol significantly increased the NO indices. Thus it remains possible that NO is playing a role via mechanisms that are independent of its anti-proliferative effects.

The functional significance of vascular remodeling of the afferent arterioles in L-NAME-induced hypertension is unknown. On the one hand, it may be a maladaptive response that promotes renal hypoperfusion and injury (unpublished preliminary data; ASN abstract, 2012), while contributing to the maintenance of HTN, as previously suggested. On the other hand, it may be adaptive and serve to protect the glomerulus against the elevated blood pressure. However, this adaptive response would be at the expense of an increased risk of acute renal failure if renal perfusion were challenged (e.g. if blood pressure drops rapidly). Moreover, if remodeling is an adaptive response, then it may be potentially injurious to the kidney if one decreases preglomerular remodeling without achieving good blood pressure control (as in this study); this would increase glomerular pressure and thus promote renal injury. Consequently, further studies are needed to further elucidate the mechanisms and consequences of preglomerular vascular remodeling, as well as the evolution and potential sequelae when treating it.

In conclusion, this study demonstrated that L-NAME-induced hypertension is associated with an inward eutrophic remodeling of the renal afferent arterioles and glomerular damage in the setting of increased cortical oxidative stress and decreased NO. Reducing oxidative stress with tempol, at a dose that did not significantly decrease blood pressure, blunted afferent arteriolar remodeling, suggesting that the interaction between NO and oxidative stress may play a major role in the pathogenesis of vascular remodeling in renal resistance vessels. The roles of other factors (e.g. angiotensin II) that may also play a role in L-NAME-induced vascular remodeling require further study.

Declaration of interest

The authors report no conflicts of interest. The authors alone are responsible for the content and writing of this article.

References

1. Kawabe K, Watanabe TX, Shiono K, Sokabe H. Influence on blood pressure of renal isografts between spontaneously hypertensive and normotensive rats, utilizing the F1 hybrids. Jpn Heart J 1978;19: 886–94.
2. Rettig R, Folberth C, Kopf D, et al. Role of the kidney in the pathogenesis of primary hypertension. Clin Exp Hypertens 1990; 12:957–1002.

3. Rettig R, Folberth CG, Stauss H, et al. Hypertension in rats induced by renal grafts from renovascular hypertensive donors. Hypertension 1990;15:429–35.
4. New DI, Chesser AM, Thuraisingham RC, Yaqoob MM. Structural remodeling of resistance arteries in uremic hypertension. Kidney Int 2004;65:1818–25.
5. Lau C, Sudbury I, Thomson M, et al. Salt-resistant blood pressure and salt-sensitive renal autoregulation in chronic streptozotocin diabetes. Am J Physiol Regul Integr Comp Physiol 2009;296: R1761–70.
6. Eftekhari A, Mathiassen ON, Buus NH, et al. Changes in blood pressure and systemic vascular resistance do not predict microvascular structure during treatment of mild essential hypertension. J Hypertens 2012;30:794–801.
7. Masulli M, Mancini M, Liuzzi R, et al. Measurement of the intrarenal arterial resistance index for the identification and prediction of diabetic nephropathy. Nutr Metab Cardiovasc Dis 2009;19:358–64.
8. Imig JD. Afferent arteriolar reactivity to angiotensin II is enhanced during the early phase of angiotensin II hypertension. Am J Hypertens 2000;13:810–18.
9. Kimura K, Tojo A, Matsuoka H, Sugimoto T. Renal arteriolar diameters in spontaneously hypertensive rats. Vascular cast study. Hypertension 1991;18:101–10.
10. Gattone II VH, Evan AP, Willis LR, Luft FC. Renal afferent arteriole in the spontaneously hypertensive rat. Hypertension 1983; 5:8–16.
11. Skov K, Mulvany M, Korsgaard N. Morphology of renal afferent arterioles in spontaneously hypertensive rats. Hypertension 1992; 20:821–7.
12. Anderson WP, Kett MM, Evans RG, Alcorn D. Pre-glomerular structural changes in the renal vasculature in hypertension. Blood Pressure 1995;2:74–80.
13. Zou LX, Imig JD, Von Thun AM, et al. Receptor-mediated intrarenal angiotensin II augmentation in angiotensin II infused rats. Hypertension 1996;28:669–77.
14. Baumbach GL, Heistad DD. Remodeling of cerebral arterioles in chronic hypertension. Hypertension 1989;13:968–72.
15. Park J, Schiffrin E. Small artery remodeling is the most prevalent (earliest?) form of target organ damage in mild essential hypertension. J Hypertens 2001;19:921–30.
16. Fan Z-D, Zhang L, Shi Z, et al. Artificial microRNA interference targeting AT1a receptors in paraventricular nucleus attenuates hypertension in rats. Gene Ther 2012;19:810–17.
17. Joo Turoni CM, Reynoso HA, Marañón RO, et al. Structural changes in the renal vasculature in streptozotocin-induced diabetic rats without hypertension. Nephron Physiol 2005; 99:50–7.
18. Miatello R, Cruzado M, Risler N. Mechanisms of cardiovascular changes in an experimental model of syndrome X and pharmacological intervention on the renin-angiotensin system. Curr Vasc Pharmacol 2004;2:371–7.
19. Kurose I, Wolf R, Grisham MB, et al. Microvascular responses to inhibition of nitric oxide production. Role of active oxidants. Circ Res 1995:76:30–9.
20. Zhou MS, Schulman IH, Raij L. Nitric oxide, angiotensin II, and hypertension. Semin Nephrol 2004;24:366–78.
21. Rudic RD, Shesely EG, Maeda N, et al. Direct evidence for the importance of endothelium-derived nitric oxide in vascular remodeling. J Clin Invest 1998;101:731–6.
22. Mattson DL, Lu S, Nakanishi K, et al. Effect of chronic renal medullary nitric oxide inhibition on blood pressure. Am J Physiol 1994;266:H1918–26.
23. Bouriquet N, Dupont M, Herizi A, et al. Preglomerular sudanophilia in L-NAME hypertensive rats. Involvement of endothelin. Hypertension 1996;27:382–91.
24. Ribeiro MO, Antunes E, de Nucci G, et al. Chronic inhibition of nitric oxide synthesis. A new model of arterial hypertension. Hypertension 1992;20:298–303.
25. Goligorsky MS, Brodsky SV, Noiri E. NO bioavailability, endothelial dysfunction, and acute renal failure: new insights into pathophysiology. Seminars in Nephrology 2004;24:316–23.
26. De Bruno MP, Turoni CMJ, Marañón RO, et al. Structural changes in the kidney induced by coarctation hypertension. Clin Exp Hypertens 2001;23:501–11.
27. Skalli O, Ropraz P, Trzeciak A, et al. A monoclonal antibody against alpha-smooth muscle actin: a new probe for smooth muscle differentiation. J Cell Biol 1986;103:2787–96.
28. Brand M, Lamandé N, Sigmund CD, et al. Angiotensinogen modulates renal vasculature growth. Hypertension 2006;47: 1067–74.
29. Qujeq D, Habibinudeh M, Daylmkatoli H, Rezvani T. Malondialdehyde and carbonyl contents in the erythrocytes of streptozotocin-induced diabetic rats. Int J Diabetes Metabolism 2005;13:96–8.
30. Lowry OH, Rosebrough NJ, Farr AL, Randall RJ. Protein measurement with the Folin phenol reagent. J Biol Chem 1951; 193:265–75.
31. Chander V, Chopra K. Renal protective effect of molsidomine and L-arginine in ischemia-reperfusion induced injury in rats. J Surg Res 2005;128:132–9.
32. Gibbons GH, Dzau VJ. The emerging concept of vascular remodeling. N Engl J Med 1994;330:1431–8.
33. Mulvany MJ. Vascular remodeling of resistance vessels: can we define this? Cardiovascular Research 1999;41:9–13.
34. Mulvany MJ, Baumbach GL, Aalkjaer C, et al. Vascular remodeling. Hypertension 1996;28:505–6.
35. Pires PW, Deutsch C, McClain JL, et al. Tempol, a superoxide dismutase mimetic, prevents cerebral vessel remodeling in hypertensive rats. Microvasc Res 2010;80:445–52.
36. Carlström M, Lai EY, Ma Z, et al. Superoxide dismutase 1 limits renal microvascular remodeling and attenuates arteriole and blood pressure responses to angiotensin II via modulation of nitric oxide bioavailability. Hypertension 2010;56:907–13.